

An X-ray scattering and simulation study of the ordering kinetics in CuAu

K. R. ELDER¹, O. MALIS², K. LUDWIG²
B. CHAKRABORTY³ and N. GOLDENFELD⁴

¹ *Department of Physics, Oakland University
Rochester, MI 48309-4401, USA*

² *Department of Physics Department, Boston University
590 Commonwealth Ave., Boston, MA 02215, USA*

³ *Physics Department, Brandeis University - Waltham, MA 02254, USA*

⁴ *Department of Physics, University of Illinois at Urbana-Champaign
1110 West Green Street, Urbana, IL 61801, USA*

(received 11 March 1998; accepted in final form 15 July 1998)

PACS. 05.70Ln – Nonequilibrium thermodynamics, irreversible processes.

PACS. 64.60Cn – Order-disorder transformations; statistical mechanics of model systems.

PACS. 81.30Hd – Constant-composition solid-solid phase transformations: polymorphic, massive, and order-disorder.

Abstract. – A detailed numerical and experimental study of the ordering of the low-temperature tetragonal phase of CuAu is presented. The numerical simulations are based on a coarse-grained free energy derived from electronic structure calculations of CuAu, while the experimental results are obtained from *in situ* X-ray scattering. Both theoretical and experimental work indicate a subtle kinetic competition between the ordered tetragonal phase and the metastable modulated phase.

What determines the microstructure of a typical alloy? While there is no simple answer to this question it is understood [1, 2] that a variety of morphological instabilities can be encountered in non-equilibrium processing which create spatial inhomogeneities that are magnified during coarsening. In this paper experimental and theoretical techniques are combined to investigate the intricate morphologies that emerge during the sublattice ordering of the low-temperature tetragonal phase of CuAu. The results of this study indicate a subtle competition between a metastable modulated phase and the stable low-temperature ordered phase. At shallow quench temperatures or early times the modulated state is favored while at lower temperature or later times the ordered phase dominates. The results are supported by *in situ* X-ray scattering experiments and numerical simulations.

The phases of CuAu that are relevant to this study are a high-temperature disordered face-centered cubic phase, an intermediate-temperature modulated orthorhombic phase and a low-temperature ordered tetragonal phase. The modulated phase consists of a periodic array of antiphase domain walls arranged perpendicular to the tetragonal direction. The wavelength of the modulated phase is 10 underlying fcc unit cells. The transitions from the ordered phase

to the modulated phase and from the modulated phase to the disordered phase are both first order and occur at $T_{\text{OM}} = 658$ K and $T_{\text{MD}} = 683$ K, respectively. Rapid temperature quenches through these transitions can lead to many interesting morphologies. In this paper quenches to the low-temperature ordered phase (*i.e.* $T < T_{\text{OM}}$) are considered. Earlier experiments [3] suggested homogeneous nucleation for quenches just below T_{OM} and spinodal ordering for deep quenches.

In principle, the ordering kinetics involves both structural relaxation of the lattice and a local rearrangement of atoms into the appropriate sublattice. Although it is desirable to use a microscopic model that describes these two distinct processes [4,5], it is difficult to explore the length and time scales of interest in this paper with such an atomistic approach. To study these long length and time scales a mean-field continuum model [5,6] will be used. The mean-field model is based on a microscopic Hamiltonian derived from effective medium theory (EMT) [4]. EMT is a semi-empirical approach based on the concept of an electron-density-dependent contribution to the total energy of a system of atoms. The parameters of this model were fit to experimental values of the lattice parameter, bulk modulus and shear modulus of Cu and Au and to the heat of formation of the 50-50 alloy [4]. The Hamiltonian describing Cu-Au alloys through the whole concentration range is defined by the EMT functional form and these parameters. The mean-field model is obtained from this Hamiltonian and describes the free energy of the system as a functional of the sublattice concentration and explicitly assumes that the structural relaxation is instantaneous. The model predicts the existence of the phases and transitions described above. As with most mean-field theories the predictions for the transition temperatures (*i.e.* $T_{\text{MD}} = 1263$ K and $T_{\text{OM}} = 1211$ K) are not in good agreement with the experimental values [7]. An enhanced mean-field theory could be constructed to improve the quantitative details, but the competition between ordered and modulated phases predicted by the current model already agrees qualitatively with experiment.

Assuming that the kinetics are driven by minimization of this free energy, the following kinetic model can be proposed:

$$\partial\eta/\partial t = -2\Gamma(2\pi/a)^d([a_T + e(\nabla_{\perp}^2 - \nabla_{\parallel}^2) + f\nabla_{\perp}^4]\eta - 4u\eta^3 + 6v\eta^5) + \zeta, \quad (1)$$

where $\langle\zeta(\vec{r}, t)\zeta(\vec{r}', t')\rangle = -2k_{\text{B}}T\Gamma\delta(\vec{r} - \vec{r}')\delta(t - t')$ and η represents the sublattice concentration. All parameters, except Γ , the mobility, were determined by the EMT calculations described above [5] and are $a_T = 0.042(T - 1219 \text{ K}) \text{ meV/K}$, $u = 5.25 \text{ meV}$, $v = 6.1 \text{ meV}$, $e = 25.5 \text{ meV}/(2\pi/a)^2$ and $f = 195.5 \text{ meV}/(2\pi/a)^4$ and a is the shortest lattice parameter in the tetragonal structure of the low-temperature CuAu(I) ordered phase. The only temperature dependence enters through a_T . Rather than introducing a phenomenological or empirical form for Γ , all times will be recorded in terms of a Ginzburg-Landau time defined such that the fastest growing Fourier mode grows as $e^{t/t_{\text{GL}}}$. For this model $t_{\text{GL}} = 1/[2\Gamma(2\pi/a)^d(e^2/4f - a_T)]$. The subscripts \perp and \parallel refer to directions perpendicular and parallel to the ordering directions, respectively. The interesting structures develop in the plane perpendicular to the ordering direction and for computational efficiency gradients in the \parallel direction will be ignored. This model differs from the standard kinetic model of sublattice ordering (Model A) since the coefficient of the ∇_{\perp}^2 term is negative, which serves to enhance rather than suppress spatial gradients. Since it is unphysical to enhance spatial gradients on very small length scales, higher-order derivatives are needed (*i.e.* ∇_{\perp}^4). It is precisely the competition between the ∇_{\perp}^2 and ∇_{\perp}^4 that leads the selection of a finite wavelength modulated state. A simple linear stability analysis shows that the most unstable mode is at $q_0 = \sqrt{e/2f}$.

Equation (1) was simulated on a discrete lattice using Euler's method to evaluate the time derivatives and a "spherical Laplacian" introduced by Oono and Puri [8] to account for the spatial gradients. Relatively small space ($\Delta x = (2\pi/q_0)/12$) and time ($\Delta t \sim 0.004 t_{\text{GL}}$)

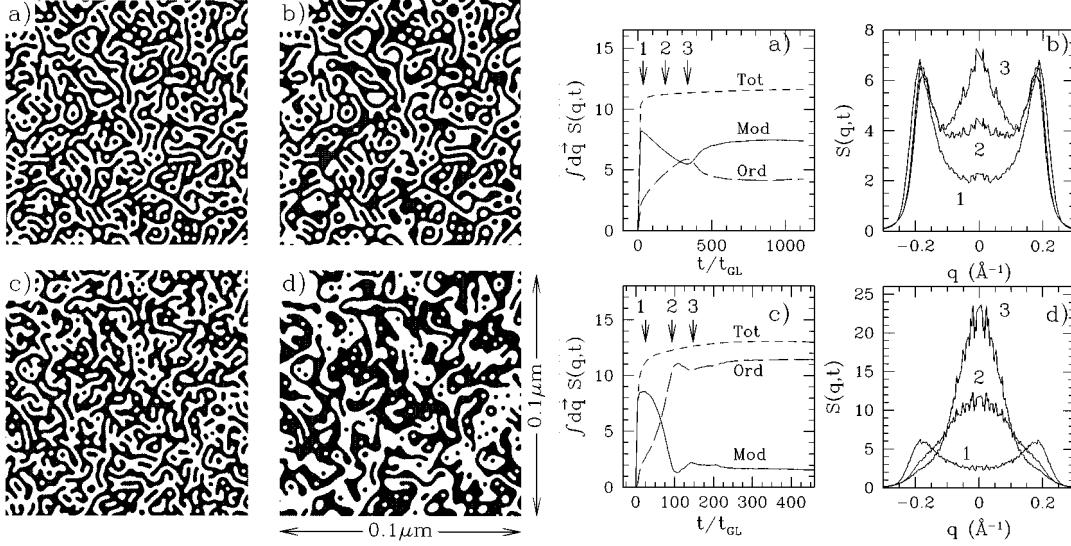


Fig. 1

Fig. 2

Fig. 1. – Transient morphologies for $T_{\text{OM}} - T = 5$ K and 15 K obtained from numerical simulations. The light and dark regions correspond, respectively, to $\eta < 0$ and $\eta > 0$. Only one twenty-fifth of the full simulation cell ($0.5 \mu\text{m} \times 0.5 \mu\text{m}$) is shown here. Figures (a) and (b) correspond to $T_{\text{OM}} - T = 5$ K at times $t/t_{\text{GL}} = 112$ and 375, respectively. Figures (c) and (d) depict η for $T_{\text{OM}} - T = 15$ K at times $t/t_{\text{GL}} = 49$ and 146, respectively.

Fig. 2. – In figures (a) and (c) the numerical simulated integrated intensities are shown as a function of time for quenches to $T_{\text{OM}} - T = 5$ K and $T_{\text{OM}} - T = 15$ K, respectively. The solid, long-dashed and short-dashed lines correspond to the modulated, ordered and total integrated intensities respectively. In figures (b) and (d) sample structure factors are shown at $T_{\text{OM}} - T = 5$ K and $T_{\text{OM}} - T = 15$ K, respectively at the times indicated by the arrows in (a) and (c). The lines from bottom to top at $q = 0$ correspond to the earliest to latest times.

steps and large system sizes were used to eliminate spurious numerical effects. Equation (1) was simulated on a system of dimension 2048×2048 grid points corresponding to a physical dimension of $0.5 \mu\text{m} \times 0.5 \mu\text{m}$.

The three equilibrium phases, disordered, modulated and ordered, are described by $\langle \eta \rangle = 0$, $\eta \approx A \sin(q_0 \vec{r} \cdot \hat{n})$ and $\langle \eta \rangle = \eta_0$, respectively, where \hat{n} is an arbitrary unit vector in the ordering plane and q_0 is the modulation wave vector. This differs from CuAu for which the modulation wave vector appears only along the Bravais lattice directions in the ordering plane. Transmission electron microscope work [9, 10] has indeed shown that the morphologies in the modulated regime are quite anisotropic. Nevertheless, even at this level of simplification the model contains many complexities that are important to the ordering process. Most importantly, it incorporates the subtle competition between the modulated, disordered and ordered phases.

To examine the kinetics of ordering below T_{OM} several simulated quenches were examined. In the first set of quenches the system was equilibrated in the disordered phase (*i.e.* at $T - T_{\text{MD}} = 20$ K) and then instantaneously quenched to temperatures below T_{OM} . A qualitative picture of the subsequent dynamics is shown in fig. 1 for quench temperatures of $T_{\text{OM}} - T = 5$ K and 15 K. At both temperatures the very early stages are dominated by highly interconnected structures that contain many defects. The subsequent kinetics are

dominated by a coarsening in which the average length scale of the patterns increases. This coarsening occurs mainly near defects in the pattern. Figure 1 also indicates that the lower quenches coarsen more rapidly. This is due to the increase in the free-energy difference between the modulated and ordered states at lower temperatures. Although not shown here, this effect was verified at other quench temperatures (*i.e.* $T - T_{\text{OM}} = 13$ K and 65 K).

To further illustrate the kinetics of ordering and for comparison with the experimental X-ray scattering patterns it is useful to consider the spherically averaged dynamic structure factor, $S(q, t)$. $S(q, t)$ is defined as

$$S(q, t) \equiv \frac{\sum_{q^2=q_x^2+q_y^2} |\eta(\vec{q}, t)|^2}{\sum_{q^2=q_x^2+q_y^2} 1}, \quad (2)$$

where $\eta(\vec{q}, t)$ is the discrete Fourier transform of $\eta(\vec{x}, t)$. The ordered and modulated phases are represented by a peak(s) in $S(q, t)$ centered around $q_{\text{O}} = 0$ and $q_{\text{M}} = \pm 1.8/\text{\AA}$, respectively. To examine the competition between the two phases the structure factor was fit to two symmetric peaks: an ordered peak, $S_{\text{O}}(k, t)$, and a modulated peak, $S_{\text{M}}(k, t)$, centered around q_{O} and q_{M} , respectively. For comparison with experiment the integrated intensities (*i.e.* $\int d\vec{q} S_{\text{O}}(q, t)$ and $\int d\vec{q} S_{\text{M}}(q, t)$) were evaluated for each peak. Ideally, these quantities reflect the volume fraction of the two phases. In practice there is no clear distinction between “ordered” and “modulated” regimes as is illustrated in morphological patterns shown in fig. 1. Nevertheless these quantities are useful for comparison with experiment as they are relatively insensitive to experimental resolution (which is not the case for peak heights and widths). The dynamics of the integrated intensities and some representative structure factors are shown in fig. 2.

The structure factors in fig. 2 indicate that satellite peaks are generated at early times for quenches just below T_{OM} consistent with the highly interconnected patterns shown in figs. 1a and 1c. The metastability of the modulated phase is highlighted by the persistence of the satellite peaks at late times as seen in figs. 2a and 2b. At the lower quench temperature (see figs. 2c and 2d) the central peak associated with the ordered phase dominates more rapidly.

To test the numerical predictions and to provide additional insight into the ordering, X-ray scattering studies on the modulated and ordered superlattice peaks near (110) were carried out. The experiments were conducted on beamline X20C at the National Synchrotron Light Source. Several kinds of CuAu samples were studied—including bulk single crystals and polycrystalline films approximately 10 μm thick. The detailed ordering kinetics differed slightly between samples but the qualitative features have been reproduced consistently. The results presented in this paper are from the polycrystalline films. The samples were held in a He atmosphere and *in situ* X-ray diffraction patterns were recorded by a linear position-sensitive photodiode array detector every 3 s. Quench rates were typically of the order 5.5 degrees/s. Similar to the numerical simulation the prequench samples were equilibrated at $T - T_{\text{MD}} = 20$ K and then rapidly quenched to temperatures below T_{OM} . All X-ray intensities, $I(q, t)$, were normalized with the incident intensity and a linear function was subtracted from each pattern to remove the background.

The X-ray scattering results for quenches to $T_{\text{OM}} - T = 5$ K and 15 K are summarized in fig. 3 and can be compared directly with the numerical results shown in fig. 2. In this comparison it should be noted that the numerical results are for correlations in the sublattice concentration (η) which, for example, peak at $q = 0$ for the ordered phase (*i.e.* $\eta = \eta_{\text{O}}$). In the experiment the same ordered phase leads to a superlattice peak or Bragg reflection centered around $2\pi/d$, where d is the (110) plane spacing. Both experiment and simulation show that satellite peaks are generated at early times and that the persistence of these peaks is related to the quench temperature. Although not shown here, it was also found, in both experiment and simulation, that the early-stage kinetics are very similar above and below T_{OM} .

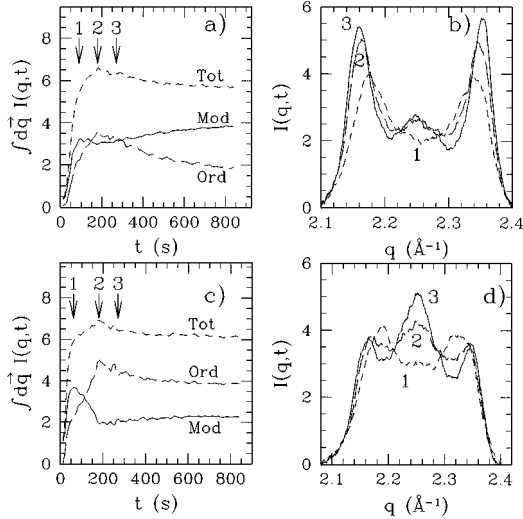


Fig. 3

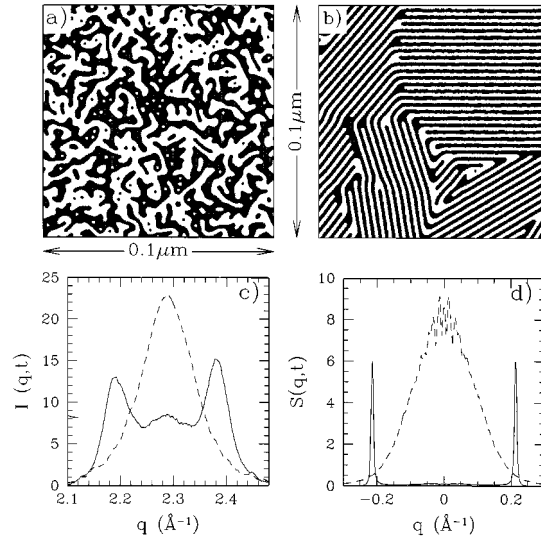


Fig. 4

Fig. 3. – In (a) and (c) the experimentally measured integrated intensities are shown as a function of time for quenches to $T_{\text{OM}} - T = 5$ K and $T_{\text{OM}} - T = 15$ K, respectively. The solid, long-dashed and short-dashed lines correspond to the modulated, ordered and total integrated intensities, respectively. In figures (b) and (d) sample scattering patterns are shown at $T_{\text{OM}} - T = 5$ K and $T_{\text{OM}} - T = 15$ K, respectively at the times indicated by the arrows in (a) and (c).

Fig. 4. – In figs. (a) and (b) configurations are shown at $t/t_{\text{GL}} = 18.8$ for quenches from disordered and partially modulated phases, respectively. As with fig. 1 only one twenty-fifth of the full simulation cell is shown. In fig. (c) the experimental scattering intensity is shown at 1650 s after the quench for both disordered (dashed line) and modulated (solid) initial states. A similar comparison is shown for the numerical structure factor in (d) at $t/t_{\text{GL}} = 18.8$ after the quench.

One feature that was observed in the experiment and not in the simulations was the shift in position with time of the X-ray peaks. This motion arises from changes in both the lattice spacing and modulation wavelength. The fundamental (200) peaks (not presented here) directly show the evolution of the lattice structure [11]. Examination of these indicates that, at the temperatures and time scales discussed below, the lattice has already relaxed to its tetragonal shape. Another significant effect is the shifting of the satellite peaks away from the central superlattice peak. These changes are typically quite large and occur in the early-to-intermediate time scales. For example in the quench to $T_{\text{OM}} - T = 15$ K the modulation wavelength decreased from approximately 15.6 to 11.5 lattice constants on a time scale of 300 s.

Diffuse scattering studies of the short-range ordered alloy have found satellites around the superlattice peaks with a “modulation” wavelength approximately 40% larger than in the equilibrium modulated state [12]. In the early stages of ordering following a quench, these satellite peaks grow rapidly in height before moving outward to the equilibrium positions.

The ordering kinetics can be strongly altered by changing the prequench state from a disordered phase to a modulated phase since, in the model, the modulated phase is metastable at low temperatures and the disordered phase is unstable. To examine this phenomenon two deep quenches were considered, one from a disordered initial condition (as before) and one from a modulated state. The numerical prequench state was created by seeding the system

with large modulated regimes and evolving the system until no disordered patches remained. The resulting pattern was a modulated state containing many defects. For comparison the prequench experimental system was equilibrated in the modulated phase at $T - T_{\text{OM}} = 3$ K.

Quenching these states to $T_{\text{OM}} - T = 65$ K led to the results illustrated in fig. 4. The influence of the prequench state can be clearly seen in figs. 4a and 4b which compare configurations at the same time following the quench. The persistence of the prequench modulation is quite apparent in fig. 4b. The erosion of this modulated phase occurs only at defects in the pattern. In principle the ordered regions can spontaneously nucleate in a purely modulated regime, however it appears that the nucleation rates are very small. For example, in one test simulation conducted at $T_{\text{OM}} - T = 65$ K no nucleation events were observed for times up to $t/t_{\text{GL}} = 5000$. This is also apparent although less obvious in the quenches described earlier (see fig. 1).

The experimental and theoretical results for these quenches are compared in figs. 4c and 4d. In fig. 4c the scattering intensity is shown at 1650 s after the quench for both prequench states. A similar comparison is provided in fig. 4d for the numerical simulations. In both experiment and simulation growth of the ordered state is seen to be strongly reduced for the modulated prequench state. This can be seen by comparing the amplitudes of the central and satellite peaks for the two different prequench states.

In summary, the combined experimental and theoretical work presented in this paper has provided a detailed description of the kinetics of ordering in the low-temperature tetragonal phase of CuAu. This description highlights the influence of the metastable modulated phase on the ordering process and the interesting kinetics that result. The continuum model provided a good qualitative prediction of the competition between the ordered and modulated phases as a function of time and pre- and post-quench temperatures.

The authors would like to thank B. KLEIN and N. GROSS for many useful discussions. The work of KE was supported by a Research Corporation Grant #CC4181. The work of BC was supported by NSF grants DMR-9208084 and DMR-952093. NG acknowledges support from NSF through grant DMR-93-14938. The Boston University component of this research was supported by NSF under DMR-9633596. The NSLS is supported by DOE Division of Materials Sciences and Division of Chemical Sciences.

REFERENCES

- [1] GUNTON J. D., SAN MIGUEL M. and SAHNI P., in *Phase Transitions and Critical Phenomena*, edited by C. DOMB and J. L. LEBOWITZ, Vol. 8 (Academic Press, New York) 1983.
- [2] BRAY A. J., *Adv. Phys.*, **32** (1994) 357.
- [3] TANAKA Y., UDOH K-I., HISATSUNE K. and YASUDA K., *Philos. Mag. A*, **69** (1994) 925.
- [4] ZHIGANG XI *et al.*, *J. Phys. Condens. Matter*, **4** (1992) 7191.
- [5] CHAKRABORTY B. and XI Z., *Phys. Rev. Lett.*, **68** (1992) 2039.
- [6] CHAKRABORTY B., ELDER K. and GOLDENFELD N., *Physica A*, **224** (1996) 113.
- [7] Monte Carlo simulations based on the same microscopic model predicted $T_{\text{OM}} = 708$ K and gave a very good description of the phase diagram (*cf.* ZHIGANG XI *et al.*, *J. Phys. Condens. Matter*, **4** (1992) 7191).
- [8] OONO Y. and PURI S., *Phys. Rev. A*, **58** (1987) 836.
- [9] OGAWA S., WATANABE D., WATANABE H. and KOMODA T., *Acta. Crystallogr.*, **11** (1958) 872.
- [10] GLOSSOP A. and PASHLEY D., *Proc. R. Soc. London, Ser. A*, **250** (1959) 132.
- [11] MALIS O. and LUDWIG K., in preparation.
- [12] MALIS O., LUDWIG K., SCHWEIKA W., BAI J., ICE G. E. and SPARKS C. J., in preparation.